ENERGETIC EFFICIENCY OF MASS TRANSFER ACCOMPANIED BY CHEMICAL REACTIONS IN LIQUID-LIQUID SYSTEMS

Magdalena Jasińska[*], Jerzy Bałdyga

Warsaw University of Technology, Faculty of Chemical and Process Engineering, ul. Waryńskiego 1, Warsaw, Poland

Energetic efficiency depicting the fraction of energy dissipation rate used to perform processes of drop breakup and mass transfer in two-phase, liquid-liquid systems is considered. Results of experiments carried out earlier in two types of high-shear mixers: an in-line rotor-stator mixer and a batch rotor-stator mixer, have been applied to identify and compare the efficiency of drop breakage and mass transfer in both types of mixers. The applied method is based on experimental determination of both: the product distribution of chemical test reactions and the drop size distributions. Experimental data are interpreted using a multifractal model of turbulence for drop breakage and the model by Favelukis and Lavrenteva for mass transfer. Results show that the energetic efficiency of the in-line mixer is higher than that of the batch mixer; two stator geometries were considered in the case of the batch mixer and the energetic efficiency of the device equipped with a standard emulsor screen (SES) was higher than the efficiency of the mixer equipped with a general purpose disintegrating head (GPDH) for drop breakup but smaller for mass transfer.

Keywords: chemical test reactions, energetic efficiency of mixing, mass transfer, liquid-liquid system, rotor-stator mixer

1. INTRODUCTION

In this paper drop breakage and mass transfer accompanied by complex chemical reactions carried out in in-line and batch rotor-stator devices are considered. Rotor-stator devices are used in many technologies in the chemical, pharmaceutical, biochemical, agricultural, cosmetic, health care and food processing industries. They belong to the group of high-shear devices and are characterized by a focused delivery of energy to active high-shear regions that occupy very a small fraction of internal mixer space. High stresses and high shear rates are generated in rotor-stator mixers because the rotor is situated in a close proximity of the stator and very high rotor speeds are applied. Such delivery of energy results in fast breakage of droplets and intensive mass transfer in the small active region of the mixer but the same time there is slow mass transfer and no breakage in larger regions characterized by a low rate of energy dissipation. Creation of high shear requires applying high agitation power and thus it is important to check how efficiently this power is used. This means that development of methods that can be used to predict the agitation power, to estimate both the efficiency of drop breakage and the efficiency of mass transfer is of importance. Moreover, to characterize properly mass transfer one needs to apply reliable models.

The energy dissipation rate in the in-line rotor-stator mixer resulting from agitation and flow can be calculated from the power number equation in the form proposed by Baldyga et al. (2007) and published for considered Silverson 088/150 MS mixer by Hall et al. (2013) as

---

$$N_P = 6.9 \cdot N_Q + 0.252 \tag{1}$$

where

$$N_Q = Q \big/ \left(N D_{out}^3 \right) \tag{2}$$

represents dimensionless flow rate or the dimensionless pumping capacity of the rotor-stator device.

In the case of batch mixers instead of Eq. (1) one should use a constant value of the power number, N_P; for considered in present work batch mixers one has $N_P = 1.7$ for the device equipped with a general purpose disintegrating head (GPDH) and $N_P = 2.3$ when a standard emulsor screen (SES) is used (Utomo, 2009; Padron, 2001).

The average rate of energy dissipation is given by Eq. (3)

$$\varepsilon_T = N_P N^3 D_{out}^5 \big/ V_H \tag{3}$$

One can see that in the case of the in-line mixer the average rate of energy dissipation, ε_T, increases with increasing both the rotor speed and the pumping capacity of the rotor-stator, Q, and in the case of batch mixer it depends on the rotation speed similarly as in the case of batch stirred tanks.

The maximum stable drop size d_d can be estimated including intermittency effects using equation given by Bałdyga and Podgórska (1998):

$$d_d = C_x^{1.54} L \left(\frac{\sigma}{\rho_c \varepsilon^{2/3} L^{5/3}} \right)^{0.93} \tag{4}$$

where L is the integral scale of turbulence and $C_x = 0.23$.

The method to characterize mass transfer is based on identifying effects of mass transfer on the product distribution of complex test reactions, applied as reactive tracers to two-phase, liquid-liquid systems. As a system of test reactions a set of two parallel reactions is used

$$A + B \xrightarrow{k_1} R, \quad A + C \xrightarrow{k_2} S \tag{5}$$
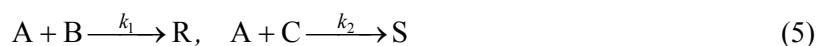
the first of them being instantaneous and the second one fast relative to mixing and mass transfer. Two reactants, benzoic acid (B) and ethyl chloroacetate (C), initially dissolved in toluene are transferred from a dispersed, organic phase to the continuous aqueous phase, where they react with the third reactant, the same for both of them, sodium hydroxide (A). The product distribution of this set of parallel chemical reactions

$$X_S = \Delta N_C \big/ N_{C0} \tag{6}$$

where ΔN_C represents the number of ester moles reacting with NaOH and N_{C0} is the complete number of ester moles introduced into the system, is a good measure of a competition between reactions, mixing and mass transfer and can be used to identify energetic efficiency of mass transfer (Jasińska et al., 2013a).

Regarding reliable prediction of the mass transfer coefficient to or from spherical particles, starting from works of Levich (1962) and Batchelor (1980) there are two basic methods available in the chemical engineering and fluid mechanics literature that are applied for modeling of mass transfer at small values of the particle Reynolds number resulting from small particle size. The first method considers surface mobility but neglects fluid deformation (so neglects velocity variation in the vicinity of droplet), whereas the second method neglects surface mobility but takes into account deformation of fluid. The first method is applied to describe external mass transfer of bubbles and not very viscous

434

liquids (Levich, 1962) and predicts $\mathrm{Sh} \propto \mathrm{Pe}^{1/2}$, the second one predicts $\mathrm{Sh} \propto \mathrm{Pe}^{1/3}$ and is applied to model mass transfer between ambient fluid and solid particles, very viscous drops or drops with immobilized surface, under assumptions that droplets behave as hard spheres. The spherical particle shape was assumed in both cases. Moreover, mass transfer models do not converge at infinitely high viscosity of dispersed phase; in correlation derived for drop dependence $\mathrm{Sh} \propto \mathrm{Pe}^{1/2}$ is conserved at infinitely large viscosity of the dispersed phase, μ_d.

Favelukis and Levrenteva (2013) included effects of drop deformation to the shape of prolate ellipsoid by using the Taylor deformation parameter:

$$\mathrm{Sh} \cdot A^* = \frac{k_L a_{drop}}{4\pi R_{eq} D_i} = \sqrt{\frac{3}{2\pi(1+K)}}\left[1 - \frac{4(4+31K)Y}{315(1+K)}N_{Ca}\right]\mathrm{Pe}^{1/2} \tag{7}$$

where $Y = (19K + 16)/(16K + 16)$, K is the viscosity ratio $K = \eta_d/\eta_c$, $\mathrm{Pe} = \dot{\gamma}R_{eq}^2/D_i$, and the capillary number is defined by $N_{Ca} = \eta_c \dot{\gamma} R_{eq}/\sigma$. R_{eq} represents the equivalent radius, i.e. the radius of a sphere of equal volume to that of the deformed drop and A^* is the ratio of the surface area of deformed drop surface area a_{drop} to the area of equivalent sphere, $4\pi R_{eq}^2$.

Equation (7) describes mass transfer to or from spherical drops. Notice that the exponent on Pe is equal to 0.5 and is independent of the viscosity ratio, and for $K = \eta_d/\eta_c \to \infty$ the mass transfer coefficient becomes equal to zero!

Problems related to mass transfer modeling with an exponent on the Péclet number varying between 1/2 and 1/3 when the viscosity ratio increases from zero to infinity were considered in our previous publications (Bałdyga and Jasińska, 2011; Jasińska et al., 2013) and some adequate models were developed. Unfortunately, they are too complex for direct use. Based on the results of Bałdyga and Jasińska (2011) the exponent on Pe in Eq.(7) can be approximated by a term $1/2 - \exp\left(-4/K^2\right)/6$, yielding:

$$\mathrm{Sh} \cdot A^* = \frac{k_L a_{drop}}{4\pi R_{eq} D_i} = \sqrt{\frac{3}{2\pi(1+K)}}\left[1 - \frac{4(4+31K)Y}{315(1+K)}N_{Ca}\right]\mathrm{Pe}^{\frac{1}{2}-\frac{exp\left(-4/K^2\right)}{6}} \tag{8}$$

Then the model describes relations between fluid deformation rate, drop deformation, surface mobility, molecular diffusion and mass transfer rate.

The aim of this study is to compare energetic efficiency of drop breakage and mass transfer processes carried out in in-line and batch rotor-stator mixers using complex test reactions and the presented above model of mass transfer. Energetic efficiency should illustrate the ratio of the minimum rate of energy dissipation necessary to perform a considered process to the experimentally measured one, and can be expressed by the ratio of time constants using a reliable reference model for mass transfer as presented in Section 3.

2. EXPERIMENTAL INVESTIGATIONS

In the case of in-line experiments (Jasińska et al., 2013a; 2016) the experimental rig consisted of a system for supply of an aqueous solution of NaOH from a constant head tank, the Silverson 088/150 MS mixer and a valve on the outflow to control the flow. The Silverson rotor-stator mixer (Silverson Machines Ltd., Chesham, UK) fitted with double concentric rotors enclosed between concentric double stators was used. The experimental rig and the Silverson mixer are shown in Figs. 1 and 2, while the mixer characteristics are presented in Table 1.
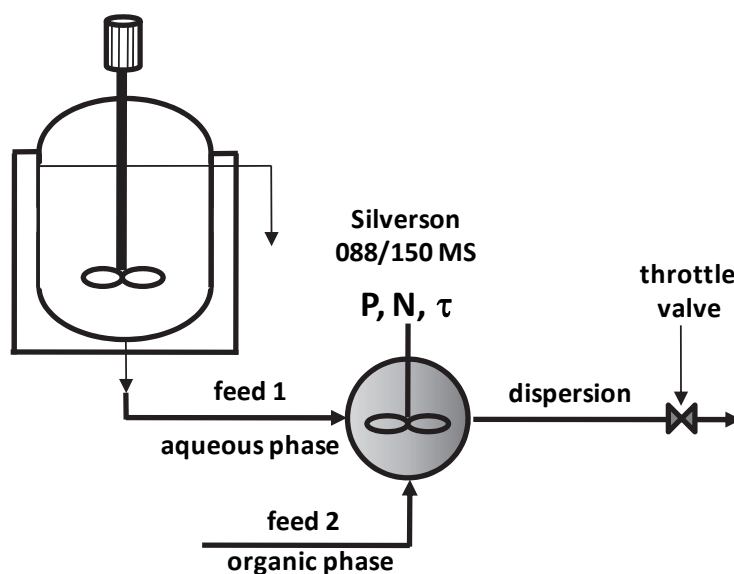
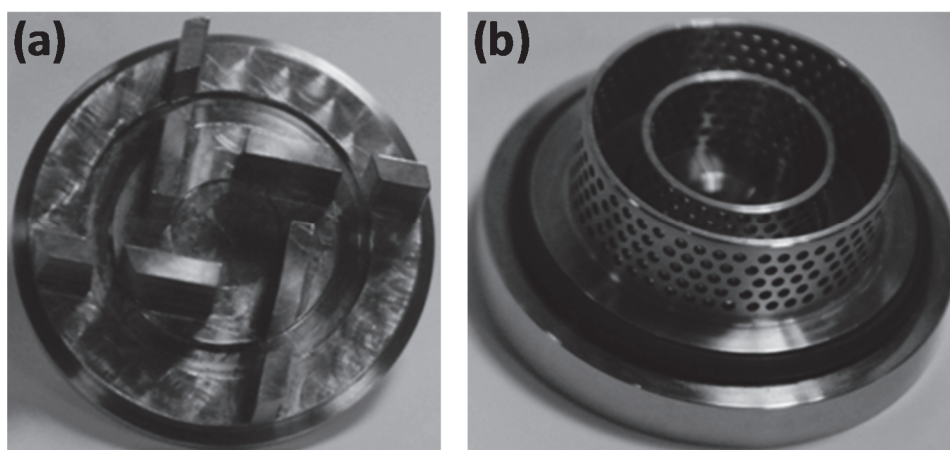Fig. 1. Silverson 088/150 MS mixer – scheme of experimental system

Fig. 2. Double rotors (a) and double emulsor stators (b)

Table 1. Dimensions of the laboratory scale in-line Silverson 088/150 MS mixer

Silverson rotor-stator (088/150 MS) parameters:	Value
D_{out}, mm	38.1
D_{in}, mm	22.4
V_H, mm^3	12655
$N_{r,out}$	4
$N_{r,in}$	4
$H_{r,out}$	240
$H_{r,in}$	180
A_{out}, mm^2	1736
A_P, %	27.4
N, rpm	150 - 11000

The instrumentation included a torque meter. The natural pumping action of the Silverson mixer was used to provide the main flow of the aqueous solution and measured by a Micro Motion Coriolis

R-Series mass flowmeter, whereas the organic solution was introduced using the syringe pump through the separate inlet. Investigations were performed for the rotation speeds ranging from 250 to 10,000 rpm for 3 values of the flow rate: Q_{aq} = 3.32×10^{-6} m^3/s, Q_{org} = 3.33×10^{-8} m^3/s (Case 1), Q_{aq} = 8.26×10^{-6} m^3/s, Q_{org} = 8.33×10^{-8} m^3/s (Case 2), and Q_{aq} = 1.65×10^{-5} kg/s, Q_{org} = 1.67×10^{-7} m^3/s (Case 3), respectively.
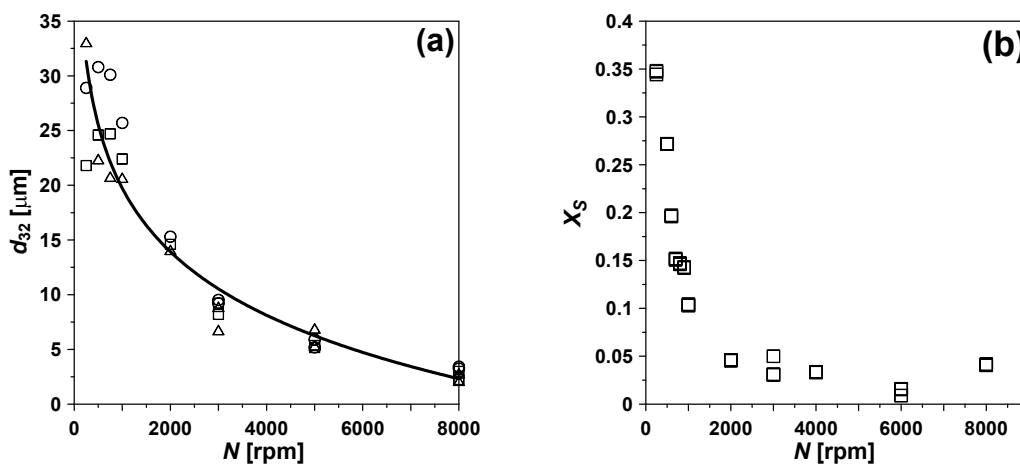

Fig. 3. Examples of experimental results for in-line mixer: (a) effect of the rotor speed on the drop size for Case 1, (b) effect of rotor speed on product distribution X_S for Case 3

In experiments the continuous phase was an aqueous solution of NaOH (A) and the dispersed phase was a solution of benzoic acid (B) and ethyl chloroacetate (C) in toluene. Feed concentrations of reactants used in experiments are presented in Table 2 together with flow rates.

Table 2. Process conditions for Cases 1, 2 and 3

	Q_{aq} [m^3/s]	Q_{org} [m^3/s]	C_{B0} [mol/m^3]	C_{C0} [mol/m^3]	C_{A0} [mol/m^3]
Case 1	3.32×10^{-6}	3.33×10^{-8}	500	500	5
Case 2	8.26×10^{-6}	8.33×10^{-8}	500	500	5
Case 3	1.65×10^{-5}	1.67×10^{-7}	500	500	5

In experiments carried out in a batch system NaOH solution (990 cm^3) was present in the vessel and the organic solution (10 cm^3) was added to start the process (Jasińska et al., 2013). Experiments were carried out in a batch reactor with a diameter of 12 cm, equipped with the Silverson rotor-stator mixer (Fig. 4a). The Silverson mixer was equipped with a four blade rotor with a diameter of 31.2 mm and a height of 12.45 mm, and two stator geometries were investigated: a standard emulsor screen (SES) (Fig. 4b) and a general purpose disintegrating head (GPDH) (Fig. 4c).

An aqueous solution of NaOH (A) of the concentration of 0.005 mol/dm^3 and a solution of benzoic acid (B) and ethyl chloroacetate (C) in toluene, both of the concentration of 0.5 mol/dm^3 were applied. The volume fraction of organic phase was 0.01.

In both cases temperature was measured using PT100 probes and all data logged on to an Emersons Delta V system. The product distribution of test reactions was determined based on high-performance liquid chromatography (HPLC) measurements. The drop size distribution was measured with the Malvern MasterSizer 3000. A surfactant Sodium Laureth Sulfate (SLES) was added to samples after carrying out the process of mixing with a chemical reaction to stabilize dispersion and avoid possible effects of droplet coalescence. In the case of droplet dispersion without a chemical reaction, SLES (0.5 wt. %) was added to water before drop dispersion experiment.

www.czasopisma.pan.pl PAN www.journals.pan.pl

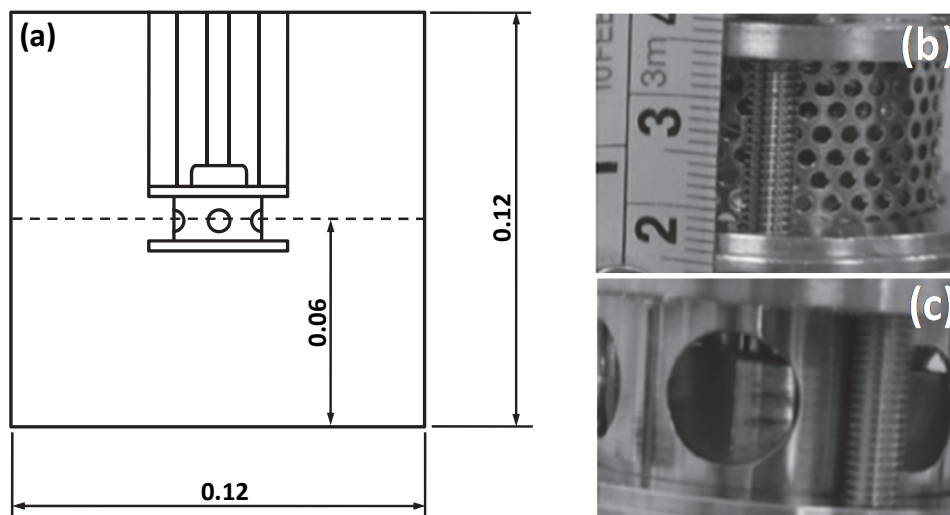*M. Jasińska, J. Bałdyga, Chem. Process Eng., 2017, 38 (3), 433-444*

Fig. 4. Batch system, experimental setup: a) rotor-stator in batch system, b) standard emulsor screen (SES), c) general purpose disintegrating head (GPDH)
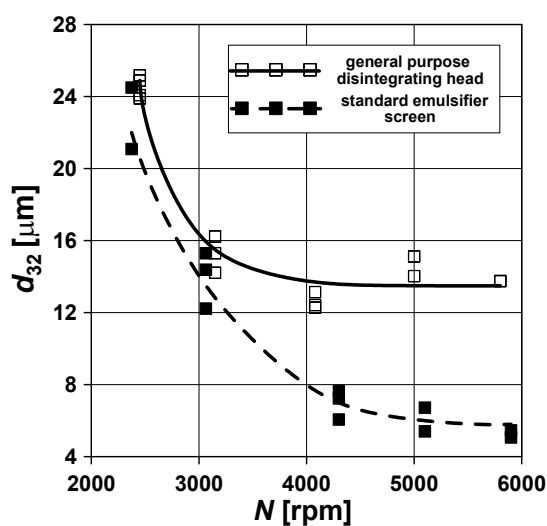

Fig. 5. Effect of rotor speed on the drop size. Silverson batch system. Vessel equipped with rotor-stator homogenizer. Comparison of results obtained with GPDH and SES screens
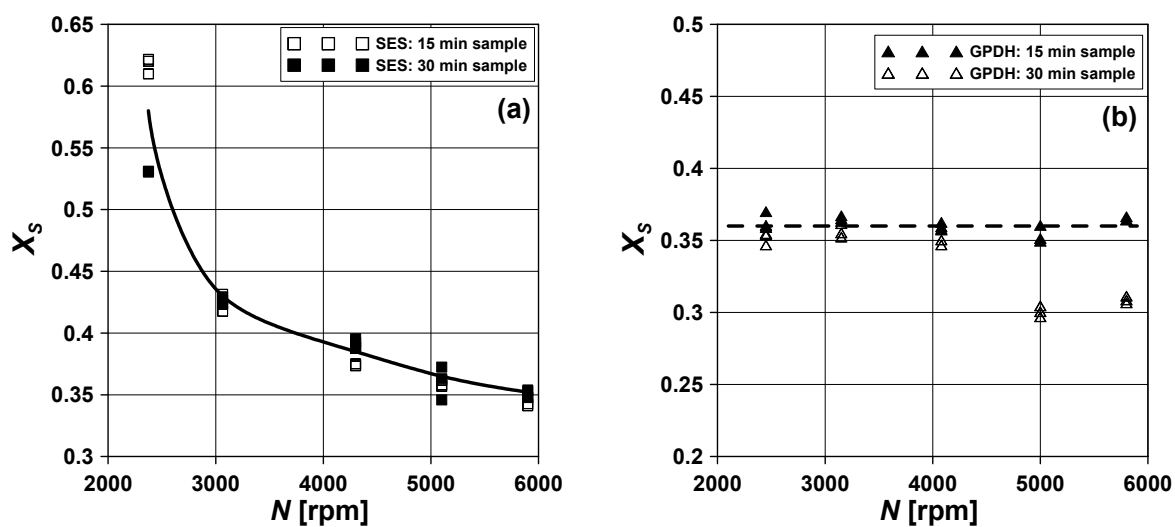

Fig. 6. Effect of rotor speed on variation of product distribution, X_S: Silverson batch system. (a) standard emulsor screen (SES), (b) general purpose disintegrating head (GPDH)

Examples of experimental data are presented in Figs. 5 and 6. The range of drop size variation observed in Fig. 5 is similar to that observed by Rueger and Calabrese (2013) for drop breakup in the Silverson L4R Batch rotor–stator mixer.

3. ENERGETIC EFFICIENCY OF DROP BREAKUP AND MASS TRANSFER IN LIQUID-LIQUID SYSTEMS

Energetic efficiency of the drop breakage process can be defined as a ratio of the rate of energy dissipation, ε_{min}, necessary to break droplets down to the maximum stable drop size assuming that the maximum stable drop size d_d is equal to experimentally measured one d_{32}, and the real power input per unit mass calculated from Eqs.(1) to (3). ε_{min} was calculated from Eq.(4) by substituting the measured d_{32} for d_d.
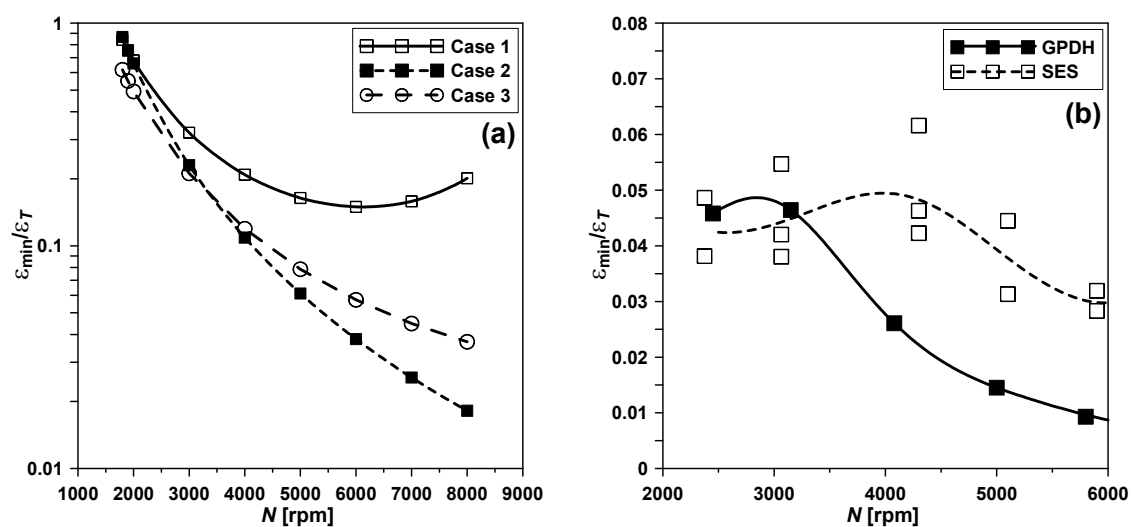

Fig. 7. Effects of rotor speed on asymptotic energetic efficiency of drop breakage (a) in-line rotor-stator mixer; (b) batch rotor-stator mixer

Figure 7 shows that the energetic efficiency is higher in the continuous flow system and decreases with increasing rotor speed and flow rate. In the case of a batch reactor efficiency is smaller and decrease of breakage efficiency with increased rotor speed is observed as well. In this case the standard emulsor screen (SES) is more efficient than the general purpose disintegrating head (GPDH).

Efficiency of mixing and mass transfer can be interpreted as a ratio of time constants for an ideal and real process (Jasińska et al., 2013b). Ideal process or reference process is one based on a reliable reference model and carried out for a constant rate of energy dissipation.

$$\text{eff} = \frac{\tau_{D,min}}{\tau_D} \tag{9}$$

Similarly to E-model having been chosen to be a reference model for mixing in homogeneous systems (Malecha et al., 2009; Jasińska et al., 2013b), one can choose a reliable reference model for mass transfer. In this paper the value of $k_L a$ will be calculated using a modified model of Favelukis and Levrenteva (2013), Eq. (7).

Efficiency of drop breakage can be expressed by an effect of drop size on the time constants for mass transfer, τ_D. The time constant $\tau_{D,min}$ in Eq. (9) can be interpreted as the shortest mass transfer time calculated from the model of Favelukis and Levrenteva (2003) using the maximum stable drop size d_d,

$R_{eq} = d_d/2$. The maximum stable drop size d_d will be estimated including intermittency effects using Eq. (4) as given by Bałdyga and Podgórska (1998).

This results in

$$\tau_{D,min} = \frac{\pi d_d^3}{6\varphi\left(k_{FL}a_{drop}\right)_{R_{eq}=d_d/2}} \tag{10}$$

where φ represents the mean value of the volume fraction of the organic, dispersed phase. Similar calculations but performed for $R_{eq} = d_{32}/2$ yield the time constant τ_D

$$\tau_D = \frac{\pi d_{32}^3}{6\varphi\left(k_{FL}a_{drop}\right)_{R_{eq}=d_{32}/2}} \tag{11}$$

Efficiency of development of the interfacial area is presented in Fig. 8 for both mixers: in-line and batch. Analysis of Fig. 8 leads to the same conclusions as in case of Fig. 7.
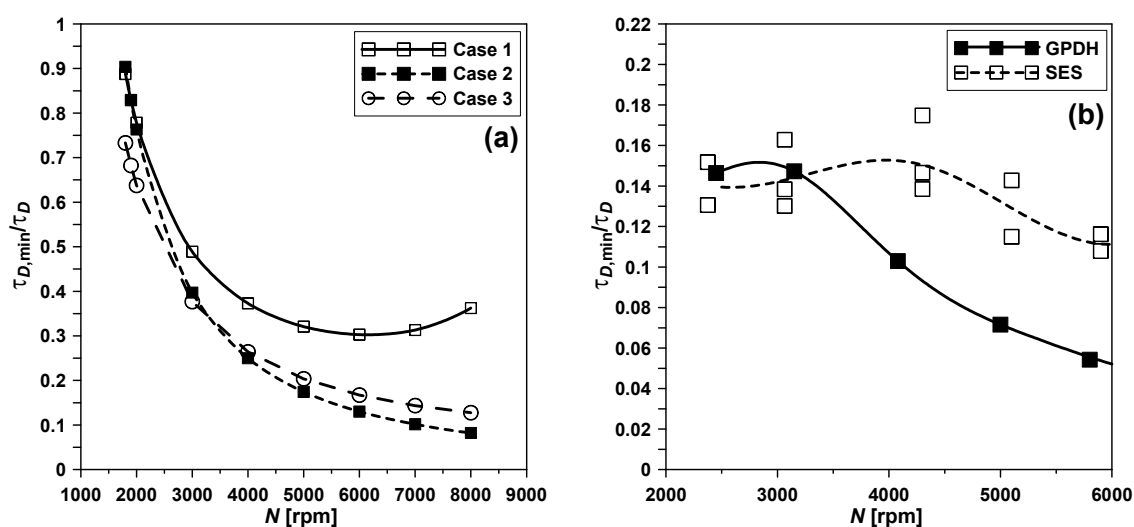

Fig. 8. Effects of rotor speed on asymptotic energetic efficiency of drop breakage based on time constant analysis: (a) in-line rotor-stator mixer; (b) batch rotor-stator mixer

Figures 3 and 6 reveal that the product distribution decreases with increasing rotor speed; in the case of the in-line mixer it increases with increasing flow rate as well, especially at a low rotor speed. Of course, increasing rotor speed gives rise to the mass transfer rate due to decreasing drop size (and so enlarging interfacial area) and increasing mass transfer coefficients. The effect of flow rate on X_S in the case of the in-line mixer results from the fact that increased flow rate decreases the residence time, which is more important at a low rotor speed, as one needs then more time for drop breakage and mass transfer. At higher values of the rotor speed N some increase of X_S with increasing N is observed in this case (Fig. 3b). The reason for this effect is most probably backmixing to the toluene feeding pipe. Faster feeding of organic phase means better protection against backmixing and observed increase of X_S is the smallest for the fastest feeding (Jasińska et al., 2016).

To interpret the observed effects the model of mass transfer with accompanying chemical reaction was applied using film theory as described by Doraiswamy and Sharma (1984). Following Jasińska et al. (2013) it was assumed that the neutralization reaction between benzoic acid (B) and NaOH (A) is instantaneous, and thus the enhancement factor can be expressed by $E = 1 + \dfrac{D_{CA}C_{A0}}{D_{CB}C_B^*}$, where D_{CA} and

D_{CB} represent diffusion coefficients for sodium hydroxide and benzoic acid respectively, C_{A0} is the bulk concentration of sodium hydroxide, and C_B^* is equilibrium concentration of benzoic acid at the drop surface.

At 20 °C $D_{CA} = 1.47 \times 10^{-9}$ m²/s and $D_{CB} = 0.91 \times 10^{-9}$ m²/s. The rate constant for alkaline ethyl chloroacetate hydrolysis is equal to $k_2 = 23$ dm³/(mol s), so the Hatta number, $\mathrm{Ha} = \sqrt{k_2 C_{A0} D_{CB}}\big/k_L$ takes values between 10^{-6} and 0.1, which means that the regime of the second reaction is between slow and very slow, and there is no reaction in the diffusion film. Other details and properties one can find elsewhere (Jasińska et al., 2013).

The film model was applied to simulate the reaction progress for a constant volume fraction of organic phase and $k_L a$ values calculated from Eq.(8) by Favelukis and Levrenteva (2013) with introducing in the present work a correction of the exponent on Pe. This correction is in fact negligible for the properties of fluids considered in this paper.

Typical results of simulations are presented in Fig. 9 for both $k_L a$ and ε, which shows how the mass transfer coefficient and the rate of energy dissipation affect the formation rate of the secondary product, S, X_S.
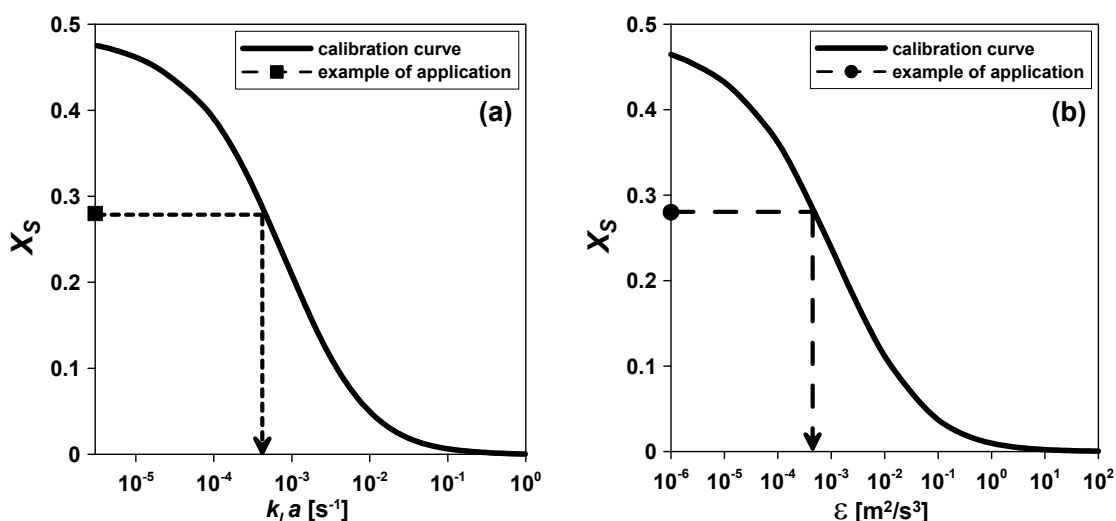

Fig. 9. Predicted effect of the mass transfer coefficient $k_L a$ the energy dissipation rate, ε, on the product distribution X_S for the batch rotor-stator experiment
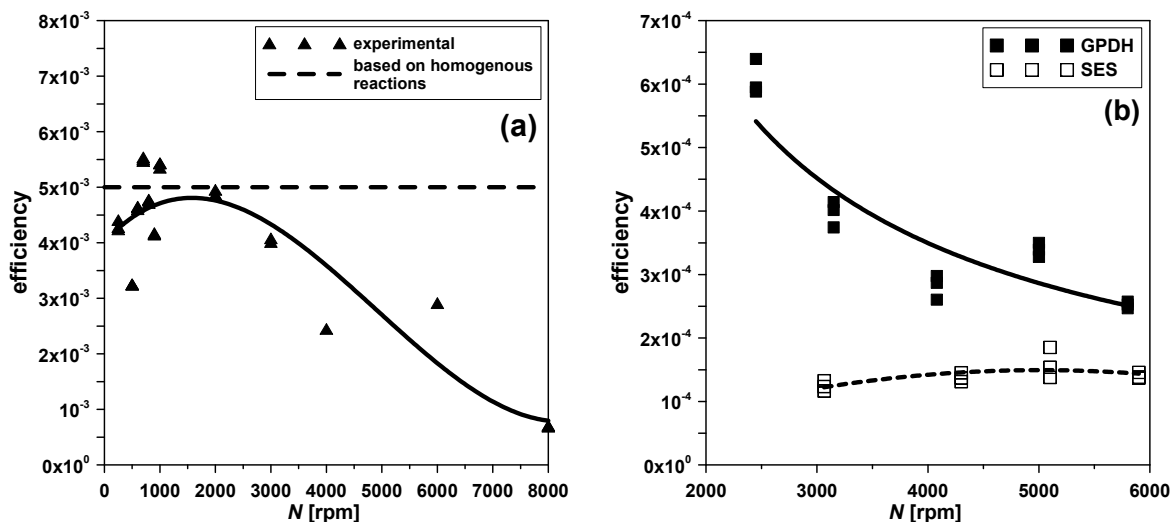

Fig. 10. Efficiency of drop brakeage and mass transfer for (a) in-line mixer system (b) batch mixer system

Figure 9 can be used in what follows as a calibration curve, which based on experimentally determined X_S values provides the smallest, "theoretical" values of the mass transfer coefficient and the rate of energy dissipation necessary to obtain experimental X_S in the batch mixer, which can be compared with the energy ε_T really used in experiment. Because both the mass transfer coefficient $k_L a$ and the energy dissipation rate, ε, depend on the rotor speed N, one can present the energetic efficiency as a function of the rotor speed as shown in Fig. 10.

For the in-line mixer experimental conditions, the calibration curve has a similar shape so it is not presented here.

Resulting efficiency is a combination of efficiencies of both, efficiency of drop breakage and mass transfer, as both of them affect the course of chemical reactions in a liquid-liquid system. A comparison of Figs. 10a and 10b leads to the following conclusions:

- The overall efficiency of drop breakage and mass transfer in the in-line mixer is one order of magnitude higher than that in the batch system. Interestingly, for the range of rotor frequency between 3000 rpm and 6000 rpm the drop size is in the range between 4 μm and 15 μm, and the efficiency of drop breakage is only slightly smaller in the batch experiment. This means that the difference is in the efficiency of mass transfer, and thus it is much smaller in the case of the batch system.

- A rotor-stator mixer equipped with a standard emulsor screen (SES) is more efficient for drop breakage than that equipped with a general purpose disintegrating head (GPDH), which is shown in Figs. 7 and 8. However, as shown in Fig. 10 the overall efficiency of the general purpose disintegrating head (GPDH) mixer is higher than that of the standard emulsor screen (SES) mixer. This means that the efficiency of mass transfer in the SES mixer is very low; the SES mixer can be used for drop breakup but should not be used to carry out mass transfer processes in liquid-liquid systems.

4. CONCLUSIONS

A method based on using complex test reactions to investigate mixing efficiency in a two-phase liquid-liquid system has been applied to compare energetic efficiency of drop breakage and mass transfer processes carried out in in-line and batch rotor-stator mixers. In this method a model of mass transfer rate based on the modified model by Favelukis and Levrenteva (2013) which includes effects of drop deformation, fluid deformation, drop surface mobility and effect of viscosity ratio has been applied to construct calibration curves for identification of mixing efficiency.

It has been shown that the energetic efficiency of the in-line rotor-stator mixer is higher than that of the batch mixer. It has been also shown that a standard emulsor screen (SES) is more efficient for drop breakage than a general purpose disintegrating head (GPDH), whereas the GDPH is more efficient for mass transfer processes. The method presented above enables one a comparison of apparatus and processes based on their energetic efficiency.

SYMBOLS

A*	surface area ratio
A_{out}	outer stator open area, m^2

A_P	fraction of outer stator open area, %
a	interfacial area per unit volume of emulsion, m^{-1}
a_{drop}	drop area, m^2
C	concentration, $mol\ m^{-3}$
C_{A0}	bulk concentration for sodium hydroxide, $mol\ m^{-3}$
C^*_B	equilibrium concentration for benzoic acid, $mol\ m^{-3}$
C_i	concentration of component "i", $mol\ m^{-3}$
D_i	molecular diffusivity of component "i", $m^2\ s^{-1}$
D_{CA}	diffusion coefficient for sodium hydroxide, $m^2\ s^{-1}$
D_{CB}	diffusion coefficient for benzoic acid, $m^2\ s^{-1}$
D_{in}	inner rotor diameter, m
D_{out}	outer rotor diameter, m
d	drop diameter, m
d_d	maximum stable drop size, m
d_{32}	Sauter diameter, m
E	enhancement factor
eff	efficiency
Ha	Hatta number, $\mathrm{Ha} = \sqrt{k_2 C_{A0} D_{CB}}/k_L$
$H_{r,in}$	number of holes in inner stator
$H_{r,out}$	number of holes in outer stator
K	viscosity ratio, $K = \eta_d / \eta_c$
k_2	rate constant of the 2nd order chemical reaction, $m^3 mol^{-1} s^{-1}$
k_L	mass transfer coefficient, $m\ s^{-1}$
L	integral scale of turbulence, m
N	rotor speed, rpm
N_{Ca}	capillary number, $\mu_c \dot{\gamma} R_{eq}/\sigma$
N_P	power number, $P/\left(\rho N^3 D_{out}^5\right)$
$N_{r,in}$	number of inner rotor blades
$N_{r,out}$	number of outer rotor blades
N_Q	dimensionless pumping capacity, $Q/\left(N D_{out}^3\right)$
P	power, W
Pe	Péclet number, $\mathrm{Pe} = \dot{\gamma} R_{eq}^2/D_i$
Q	volumetric flow rate, $m^3 s^{-1}$
R_{eq}	equivalent radius, m
Sh	Sherwood number, $k_L R_{eq} / D_i$
V_H	rotor swept volume, m^3
X_S	product distributions of complex reactions
Y	deformation parameter in Eqs. (7) and (8)

Greek symbols

ε	rate of energy dissipation, $m^2 s^{-3}$
$\dot{\gamma}$	rate of shear, s^{-1}
ν	kinematic viscosity, $m^2 s^{-1}$
η_i	viscosity of "i" phase, Pa s
ρ_i	density of "i" phase, $kg\ m^{-3}$
σ	interfacial tension, $N\ m^{-1}$
τ_D	time constant for mass transfer, s

REFERENCES

Bałdyga J. and Podgórska W., 1988. Drop break-up in intermittent turbulence. Maximum stable and transient sizes of drops. *Can. J. Chem. Eng.*, 76, 456-470. DOI: 10.1002/cjce.5450760316.

Bałdyga J., Jasińska M., 2011. Effect of model structure on complex liquid-liquid heterogeneous reactions. *Proceedings of the third European Process Intensification Conference*, EPIC2011, 20-23 June 2011, Manchester, UK, 175-181.

Bałdyga J., Kowalski A., Cooke M., Jasińska M., 2007. Investigations of micromixing in a rotor-stator mixer. *Chem. Process Eng.,* 28 (4), 867-877.

Batchelor G.K., 1980. Mass transfer from a particle suspended in turbulent fluid. *J. Fluid Mech.*, 98, 609-623. DOI: 10.1017/S0022112080000304.

Doraiswamy L.K., Sharma M.M., 1984. *Heterogeneous reactions: Analysis, examples, and reactor design. Vol. 2: Fluid-fluid-solid reactions.* Wiley, New York.

Favelukis M., Lavrenteva O.M., 2013. Mass transfer around prolate spheroidal drops in an extensional flow. *Can. J. Chem. Eng.*, 91, 1190-1199. DOI: 10.1002/cjce.21727.

Hall S., Pacek A., Kowalski A.J., Cooke M., Rothman D., 2013. The effect of scale and interfacial tension on liquid–liquid dispersion in in-line Silverson rotor–stator mixers. *Chem. Eng. Res. Des.*, 91, 2156-2168. DOI: 10.1016/j.cherd.2013.04.021.

Jasińska M., Bałdyga J., Cooke M., Kowalski A., 2016. Mass transfer and chemical test reactions in the continuous-flow rotor-stator mixer. *Theor. Found. Chem. Eng.*, 50, 901-906. DOI: 10.1134/S0040579516060075.

Jasińska M., Bałdyga J., Cooke M., Kowalski A.J., 2013a. Investigations of mass transfer with chemical reactions in two-phase liquid-liquid systems. *Chem. Eng. Res. Des.*, 91, 2169-2178. DOI: 10.1016/j.cherd.2013.05.010.

Jasińska M., Bałdyga J., Cooke M., Kowalski A.J., 2013b. Application of test reactions to study micromixing in the rotor-stator mixer (test reactions for rotor-stator mixer). *Appl. Therm. Eng.*, 57, 172-179. DOI: 10.1016/j.applthermaleng.2012.06.036.

Jasińska M., Lewandowski P., Bałdyga J., 2013. Nowy model wnikania masy z reakcją chemiczną w układach heterofazowych ciecz-ciecz. *Inżynieria i Aparatura Chemiczna*, 52 (4), 325-327.

Levich V.G., 1962. *Physical hydrodynamics*. Prentice-Hall, Englewood Cliffs, N.J.

Malecha K., Golonka L.J., Bałdyga J., Jasińska M., Sobieszuk P., 2009. Serpentine microfluidic mixer made in LTCC. *Sens. Actuators B: Chem.*, 143, 400-413. DOI: 10.1016/j.snb2009.08.010.

Padron G.A., 2001. *Measurement and comparison of power draw in batch rotor-stator mixers*. M.Sc. Thesis, University of Maryland, College Park, MD, USA.

Reuger P., Calabrese R.V., 2013. Dispersion of water into oil in a rotor-stator mixer. Part 1: Drop breakup in dilute systems. *Chem. Eng. Res. Des.,* 91, 2122-2133. DOI: 10.1016/j.cherd.2013.05.018

Utomo A.T., 2009. *Flow patterns and energy dissipation rates in batch rotor-stator mixers*. PhD Thesis, School of Engineering, The University of Birmingham, Edgbaston, UK.